Solid Earth Discuss., 5, 2043–2079, 2013
www.solid-earth-discuss.net/5/2043/2013/
doi:10.5194/sed-5-2043-2013

Solid Earth
Discussions
Open Access

On the complexity of surface ruptures during normal faulting earthquakes: excerpts from the 6 April 2009, L'Aquila (central Italy) earthquake (M_w 6.3)

L. Bonini[1], D. Di Bucci[2], G. Toscani[1], S. Seno[1], and G. Valensise[3]

[1]Dipartimento di Scienze della Terra e dell'Ambiente, Università di Pavia, Pavia, Italy
[2]Dipartimento della Protezione Civile, Rome, Italy
[3]Istituto Nazionale di Geofisica e Vulcanologia, Rome, Italy

Received: 13 September 2013 – Accepted: 30 October 2013 – Published: 14 November 2013

Correspondence to: D. Di Bucci (daniela.dibucci@protezionecivile.it)

Published by Copernicus Publications on behalf of the European Geosciences Union.

Abstract

Over the past few years the assessment of the earthquake potential of large continental faults has increasingly relied on field investigations. State-of-the-art seismic hazard models are progressively complementing the information derived from earthquake catalogues with geological observations of active faulting. Using these observations, however, requires full understanding of the relationships between seismogenic slip at depth and surface deformation, such that the evidence indicating the presence of a large, potentially seismogenic fault can be singled out effectively and unambiguously.

We used observations and models of the 6 April 2009, M_w 6.3, L'Aquila, normal faulting earthquake to explore the relationships between the activity of a large fault at seismogenic depth and its surface evidence. This very well-documented earthquake is representative of mid-size yet damaging earthquakes that are frequent around the Mediterranean Basin, and is somehow paradigmatic of the nature of the associated geologic evidence along with observational difficulties and ambiguities.

Thanks to available high-resolution geologic, geodetic and seismological data aided by analogue modeling, we reconstructed the full geometry of the seismogenic source in relation with surface and sub-surface faults. We find that the earthquake was caused by seismogenic slip in the range 3–10 km depth, and that the slip distribution was strongly controlled by inherited discontinuities. We also contend that faulting was expressed at the surface by pseudo-primary breaks resulting from coseismic crustal bending and by sympathetic slip on secondary faults.

Based on our results we propose a scheme for hierarchizing normal faults through which all surface occurrences related to faulting at depth can be interpreted in the frame of a single, mechanically coherent model. Appreciating such complexity is crucial to avoid severe over- or under-estimation of the local seismogenic potential.

SED
5, 2043–2079, 2013

1 Introduction

Starting in the 1980s many studies have attempted to infer the earthquake potential of large continental faults from their surface length and displacement (see Kim and Sanderson, 2005 for a review). As a result, over the past two decades several empirical relationships between earthquake magnitude and the extent of surface ruptures have been developed (e.g. Wells and Coppersmith, 1994; Wesnousky, 2008), quickly becoming the most widely used analytical tool in Earthquake Geology.

On the one hand, these relationships have certainly helped quantifying field geological observations, ultimately allowing them to be incorporated in analytical earthquake and seismic hazard assessment models (e.g. Stirling et al., 2013). In fact, the assessment of the hazard posed by large continental faults is increasingly relying on field investigations at all scales, and even a worldwide initiative for seismic hazard assessment such as the Global Earthquake Model (GEM) has "*. . . gathering all knowledge on active faults worldwide. . .*" as one of its founding pillars (http://www.globalquakemodel.org/what/seismic-hazard/active-faults-database/). On the other hand, however, these empirical relationships have also contributed to somehow obscure the complexity of the relationships between the seismogenic source at depth and its surface expression. As a reminder to geologists Nature has recently spawned a number of damaging earthquakes that turned out to have been generated by blind, hidden, or otherwise hard-to-identify faults (e.g. January 2010, Haiti, M_w 7.0; September 2010–February 2011, Darfield-Christchurch, New Zealand, M_w 7.1–6.3; October 2011, Van, eastern Turkey, M_w 7.1; July and August 2013, Blenheim-Coock Straight, New-Zealand, M_w 6.5).

The M_w 6.3, 6 April 2009 L'Aquila (Abruzzi, Central Italy) earthquake belongs to this category. Although the L'Aquila region had long been known for its high seismicity level along with most of Abruzzi, the 2009 earthquake challenged the standard approach for surface active fault identification because: (1) clearly visible surface faults, that prior to 2009 were presumed to be active, showed no genetic relationships with the seismo-

SED
5, 2043–2079, 2013

genic source, and only some showed negligible reactivation; and (2) post-earthquake field analyses documented only limited and discontinuous coseismic surface ruptures.

All in all, the surface evidence for the 2009 earthquake appears to delineate a "reversed tectonic hierarchy", such that the main seismogenic fault lies hidden beneath a blanket of clearly visible yet substantially harmless faults. This is not an entirely new observation in Italy – similar considerations were drawn for the 1997 Colfiorito, Umbria-Marche earthquakes (e.g. Basili et al., 1998) – but is somehow more surprising given the magnitude of the earthquake and its location in a region where active faults were deemed to be especially well expressed and mapped. What is the basis for this unexpected fault behavior? What are its potential implications for seismic hazard assessment? Can we derive from this earthquake a general rule to be used in other active faulting environments?

The 2009 event is currently the best documented continental extensional earthquake worldwide, and it makes a unique case for exploring the relationships between the activity of a deep seismogenic normal fault and its surface evidence in structurally complex areas. We used a wealth of high-resolution geologic, geodetic and seismological data combined with analogue modeling to reconstruct the geometry of the seismogenic rupture in relation with sub-surface and surface faults. We aimed at devising a scheme for active fault hierarchization that explains all surface outcomes of shallow crustal seismogenic faulting in the frame of a single, mechanically coherent interpretative model. Proper appreciation of such complexity forms the basis for a correct assessment of the local earthquake potential.

2 Tectonic setting: the challenge of youthful normal faulting

The Apennines exhibit a remarkably complex structure resulting from the overprinting of a number of subsequent tectonic phases (Fig. 1). In the early Mesozoic the region was part of the African passive margin of the Tethys Ocean; it hosted large carbonate platforms and intervening pelagic basins that were subsequently broken up

SED
5, 2043–2079, 2013

by E–W Triassic–Lower Jurassic extension (Calamita et al., 2011). Since the Cretaceous, the region evolved within the framework of the convergent motion between the African and European plates; east to northeast-verging thrusts along with their associated foredeep/thrust-top basins progressed toward the Adriatic foreland up to the Middle Pleistocene (Patacca and Scandone, 1989) and were subsequently dissected by strike-slip and normal faulting.

Following a major geodynamic change at ~ 800 kyr, SW–NE extension became the dominant tectonic style over the core of the Apennines (e.g. Hyppolite et al., 1994; Galadini, 1999), as demonstrated also by breakout, seismicity and crustal strain data (e.g. Montone et al., 2012; Carafa and Barba, 2013). Extension is definitely a youthful process in the Apennines, however, and proceeds at the relatively slow rate of 2–3 mm yr^{-1} (D'Agostino et al., 2011). In contrast, the core of the Apennines is undergoing vigorous regional-scale uplift at 1–2 mm yr^{-1} (D'Anastasio et al., 2006); this process induces fast exhumation and widespread differential erosion of the Meso-Cenozoic rocks comprising it, being by far more effective than extension in building and modifying the landscape. As a result of these competing processes, the Apennines landscape is largely dominated by the older compressional structures (Fig. 1), which tend to be emphasized by erosion despite their being inactive: some even simulate the typical basin-and-range landforms associated with the action of a mature normal fault, according to a process of geomorphological convergence referred to as "mimicking" (Valensise and Pantosti, 2001). In addition to that, and due to the combined effect of tectonic stress and gravity, extended terrains often exhibit a level of complexity that makes the correct hierarchization of active normal faults – or even their mere identification – extremely challenging. At the outcrop scale, a large normal fault of crustal significance, a shallow reactivated normal fault on the backlimb of older thrust sheets, or an even shallower sackung scarp may appear equally evident and similarly convincing as to the existence of a major seismogenic source.

SED
5, 2043–2079, 2013

3 The 6 April 2009 earthquake

The 6 April 2009 L'Aquila earthquake struck a seismically very active portion of the Apennines chain. It came at the culmination of a long foreshock/aftershock sequence recorded by permanent and temporary INGV seismometers (Chiarabba et al., 2009; Chiaraluce et al., 2011). The earthquake caused intensity up to IX–X MCS effects in a small number of villages located southeast of L'Aquila, but the largest number of collapsed buildings and casualties was reported in L'Aquila itself.

Extensive albeit limited surface breaks were reported by several workers over a 100 km^2 region elongated in the NW–SE direction between L'Aquila and Monticchio, about 15 km to the southeast (see detailed descriptions in Boncio et al., 2010; Emergeo Working Group, 2010; Vittori et al., 2011). The most continuous surface breaks were extensional cracks, some with a maximum net throw of a few centimeters, often seen at the top of a ∼ 10 m-high scarp formed by Quaternary continental deposits and running above the village of Paganica (Fig. 2).

The earthquake sequence is well described by an extraordinarily detailed double-difference catalogue of relocated events (3000 events with $M \geq 1.9$ from Chiaraluce et al., 2011; ∼ 64 000 events of all magnitudes from Valoroso et al., 2013). When coupled with moment tensor solutions for the largest shocks ($M_w \geq 2.7$; Herrmann et al., 2011), these data allow imaging individual faults activated during this complex sequence in great detail (Fig. 3). In the depth interval 3–4 to 10 km the aftershocks align rather regularly along a ∼ 9 km-wide, single planar surface dipping 45–50° to the SW over the entire fault length and extending for ∼ 16 km in the NW–SE direction. Some shallower aftershocks (i.e. above 3–4 km depth) are seen around the northern end of the fault; even though they are rather scattered, their locations highlight the activation of minor high-angle faults. In contrast, no shallow aftershocks are seen along the central and southern portions of the fault. Close to the upper portion of the major planar surface (at ∼ 3 km), some investigators recognized a sub-horizontal thrust plane inherited

SED
5, 2043–2079, 2013

from the Cenozoic compressional phase (e.g. Bianchi et al., 2010; Chiaraluce et al., 2011; Valoroso et al., 2013) (Fig. 3).

P and *S* wave analyses pointed out a very high velocity layer near the central portion of the earthquake rupture (Vp > 6 km s^{-1} and Vs ~ 4.2 km s^{-1}; respectively from Bianchi et al., 2010; Di Stefano et al., 2011). This high-velocity body has been interpreted either as composed by dolomitic rocks, or by partially hydrated mafic rocks between 3–4 and 10 km depth (Fig. 3), whereas in nearby areas the observed Vp an Vs values correspond with the characteristic velocities of the Meso-Cenozoic limestones and terrigenous rocks (Chiarabba et al., 2010). This complex distribution of geological units at depth shows that the stack of thrust sheets is characterized by strong lateral variations, as expected, and that the main coseismic slip patch is located within a high-velocity body (Fig. 3). Such a complexity is not surprising in view of the overall structure of the Abruzzi Apennines, that were built by progressive stacking of heterogeneous thrust sheets.

DInSAR measurements based on extensive Envisat and COSMO-SkyMed datasets constrained by scattered GPS observations revealed sizable coseismic crustal deformation resulting in bowl-shaped, gently-asymmetric surface subsidence peaking at 15–20 cm (Atzori et al., 2009; D'Agostino et al., 2012; Fig. 3). All published coseismic slip models agree that most of coseismic slip – up to 1.0 m – occurred between 9–10 to 3–4 km depth, whereas slip in the shallowest crust was found to be 0.1 m or less over most of the fault length (e.g. Atzori et al., 2009; Cheloni et al., 2010; D'Agostino et al., 2012). Shallower slip was documented only near the northern end of the fault, about 3 km to the northeast of L'Aquila and 8 km to the northwest of Paganica (Fig. 3).

The general strain pattern revealed by DInSAR analyses is seen to match the shape and the architecture of the intermontane basin that lies over the main coseismic slip patch and hosts the middle reach of the Aterno River valley (Fig. 3b), including the configuration of the buried limestone bedrock (Improta et al., 2012).

Notwithstanding the high quality of available data, the nearly 200 papers published to date about the 2009 L'Aquila earthquake have produced widely divergent seismotec-

SED
5, 2043–2079, 2013

tonic interpretations and models (see Table 5 in Vannoli et al., 2012, for a summary). These models are mainly based on three lines of evidence: seismological data (e.g. aftershock distribution), co-seismic slip patterns from the inversion of GPS and InSAR data, and field geology observations (see Vannoli et al., 2012 for a review).

For instance, the coseismic surface breaks were inherently ambiguous, as shown by the considerable scatter in the estimates of their total length and maximum throw, ranging from 2.6 to 19 km and 0 to 10 cm respectively (see Fig. 14 in Vittori et al., 2011, and Table 5 in Vannoli et al., 2012). Two of us personally observed the ruptures a few days after the mainshock, and noticed that the largest throws consistently occurred above areas where the natural topographic profile had been altered to allow the construction of small residential buildings, thus reducing the lateral confinement of the scarp material and allowing it to spread downhill.

The scarp where such fractures have been mapped was first interpreted as a fault by Bagnaia et al. (1992), who referred to it as the Paganica–San Demetrio fault system, and subsequently assumed to be a seismogenic source by Pace et al. (2006). In contrast, this scarp was referred to as an "uncertain or buried fault" in the digital version of the official Geological Map of Italy (Servizio Geologico d'Italia, 2006) and ignored by official active fault compilations (e.g. Galadini and Galli, 2000; Galadini et al., 2000).

The seismotectonic model based on geodetic data (InSAR, GPS) was obtained by inverting coseismic slip under the assumption of a perfectly planar fault reaching the surface along Paganica fault (e.g. Anzidei et al., 2009; Atzori et al., 2009; Walters et al., 2009; D'Agostino et al., 2012). Hence all modeled faults were drawn to intersect the topographic surface, without necessarily implying that coseismic slip extended to the shallowest portion of the crust (Fig. 3d). Since any variable slip analysis attempts to show where slip concentrates on the fault plane and where it tapers to zero, it is common practice to make the model fault much larger than the fault imaged by seismological data alone (9 km × 16 km in our case).

As for the fault shape, all investigators inverted coseismic slip under the assumption of a perfectly planar fault. This may not be 100 % true for every earthquake, but the

SED
5, 2043–2079, 2013

data resolution is normally insufficient to resolve minor departures from planarity (see Gori et al., 2012; Lavecchia et al., 2012, for a discussion on this topic).

The strain pattern revealed by DInSAR analyses matches well the shape and the architecture of the intermontane basin that lies over the main coseismic slip patch (Fig. 3). In itself this observation implies (1) that the local long-term tectonic strain is the result of sustained slip over the fault plane that ruptured on 6 April, and more specifically (2) that the slip pattern along the fault plane must have been nearly constant over several seismic cycles. The DInSAR-based model also shows that the largest subsidence occurred at the relatively large distance of about 5 km from the Paganica fault (Figs. 2 and 3). This circumstance implies that limited or no coseismic slip occurred along the main fault plane in the uppermost 3 km of the crust, and that tectonic strain in that volume of rock was consumed as slip along minor synthetic and antithetic faults off the main fault plane, either coseismically or as postseismic recovery (i.e. afterslip). In fact, sizable postseismic strains were revealed by DInSAR observations over a 3 km-wide corridor extending between the surface projection of the main coseismic slip patch and the trace of the Paganica ruptures (D'Agostino et al., 2012; Figs. 2 and 3), in agreement with direct evidence from terrestrial laser scanning observations (Wilkinson et al., 2010).

In summary, although most investigators agree on the primary character of the Paganica ruptures (to the point that the seismogenic source is called with the same name), a direct connection of this surface feature with the deep and seismogenic fault is neither warranted by the pattern of surface strains nor by the aftershock locations, which clearly depict fault complexity at 2–3 km depth. This complexity is interpreted as potentially arising from the intersection of the main fault with pre-existing discontinuities, the most important being an inherited thrust located at 3 km depth.

If coseismic slip of the 2009 earthquake was confined at 3–4 km depth, what is the origin of the associated surface breaks (i.e., the Paganica fault), and why is the surface fault throw so limited in size?

SED
5, 2043–2079, 2013

To shed light on the genetic relationships between the master fault at depth and surface structures we simulated the evolution of a blind normal fault using analogue models.

4 Deep and surface faulting: an analogue experiment perspective

To analyze the mid-to-long term evolution of an upward propagating blind normal fault and of the associated secondary structures related to the bending of the overlying rocks, we built a series of analogue models. We selected both wet clay and dry sand as preferred analogue materials; this choice allowed us to reproduce different aspects of faulting processes, making the most out of the characteristics of both these materials. A relatively recent study compared results obtained using wet clay and dry sand (Eisenstadt and Sims, 2005), highlighting their advantages and disadvantages. On the one hand, wet clay has been extensively used to analyze brittle deformation related to folding (e.g. Cloos, 1968; Withjack and Jamison, 1986; Withjack and Schlische, 2006; Henza et al., 2010; Miller and Mitra, 2011), and its effectiveness as analogue material has been recently stressed by new rheological tests (Cooke and van der Elst, 2012). On the other hand, dry sand is the most commonly used material to model tectonic deformation (e.g. Bonini et al., 2011) and its use allowed us to evaluate if rheological differences between the two materials (e.g. cohesion) may affect our observations. All our experiments took place in a normal gravity field.

4.1 Pre-existing mechanical discontinuities and fault evolution: wet kaolin experiments

Our first goal was to understand if and how low-angle mechanical discontinuities affect the upward propagation of a blind fault. As a clay type we used kaolin with 65 % of water content. Wet kaolin has a shear strength in the range 40 to 100 Pa (Eisenstadt and Sims, 2005; Cooke and van der Elst, 2012; Cooke et al., 2013) and its frictional

SED
5, 2043–2079, 2013

coefficient is about 0.6, so that, following well established scaling laws (e.g. Hubbert, 1937; Schellart, 2000), 1 cm in the experiment represents about 1 km in nature.

The deformation device is composed by two plates (Fig. 4); one remains fixed throughout the experiment, thus representing the footwall, whereas the other one is pulled by a stepper-motor at a rate of 0.005 mm s^{-1} and simulates hanging-wall subsidence. An experiment is stopped when the upward-propagating faults reach the surface of the model. To monitor and quantify the deformation we used D.I.C. analyses (Displacement Image Correlation), a non destructive, non-invasive, high-resolution optical technique that has the ability to reconstruct movements and flows of the experiments.

We used two experimental configurations: the first, Wet Kaolin #1 (WK1), representing a blind fault growing in a homogeneous setting; the second, Wet Kaolin #2 (WK2), similar to the previous one but with a low-angle discontinuity placed along the presumed propagating trajectory of the master fault (Fig. 4). Such pre-existing discontinuity has been reproduced by sliding an electrified blade through the analogue material. This innovative procedure, that has been successfully tested by Cooke et al. (2013), allowed us to introduce in the model very thin discontinuities that simulate pre-existing fault systems. Figure 5 shows significant steps selected from both experiments.

We analyzed with D.I.C. the response to the initial displacement along the two blocks (0.1 mm) to verify the deformation mechanisms acting in our models (Fig. 5a and b). The displacement fields show a triangular deformation zone, corresponding to the trishear zone described and modeled by several investigators (e.g. Erslev, 1991; Hardy and Ford, 1997; Jin and Groshong, 2006). The displacement field showed by two experiments during the very first deformation step is very similar, confirming that the experimental conditions are the same in both wet kaolin experiments.

As displacement proceeds, brittle and ductile deformation acting in the experiments begins to be visible. After a displacement of 10 mm, a monoclinal structure developed in both the experiments (Fig. 5c and d). In WK1, three synthetic and one antithetic extensional faults are formed at the tip of the master fault with a Mode II mechanism. As a result of bending, two crestal fractures formed with a Mode I mechanism at the

SED
5, 2043–2079, 2013

surface of the model, where tensile stress is maximum. A strain distribution analysis corroborates our observations showing two high-strain areas, a lower one and an upper one, spatially corresponding to the previously described brittle structures. At the same displacement level (10 mm) WK2 showed a different development of brittle structures (Fig. 5d). An individual upward-propagating fault stemming from the buried tip of the master fault appears more developed than those developed in WK1 and shows a higher dip angle. When this propagating fault encounters the pre-existing discontinuity it stops its propagation splitting into two minor elements. Meanwhile, minor faults are seen to displace the pre-existing low-angle plane. Also in this experiment some downward-propagating faults related to the bending develop at the surface of the model. Strain analyses confirm the previous observations highlighting a narrow zone where strain is highest; significantly, there is a sudden decrease of the strain value where the upward-propagating fault intersects the low-angle plane.

After 15 mm of displacement, in WK1 the upward-propagating fault reached the surface, connecting with one of the downward-propagating faults and showing a listric geometry (Fig. 5e); the connection of the two structures is well predicted by the strain distribution analysis. In contrast, in WK2 the downward- and upward-propagating faults do not appear to have connected for the same displacement level (Fig. 5f). This different behavior must necessarily be related to the role played by the low-angle discontinuity; a circumstance confirmed by the strain analysis, that shows that most of the deformation remains confined below the discontinuity. The rate of upward-propagation of the fault in WK2 is much slower than in WK1, and downward-propagating faults in WK2 are more developed than in the WK1.

A direct connection between upward- and downward-propagating faults is reached in WK2 after 25 mm of total displacement (Fig. 5g), 10 mm more than what was needed for WK1 (Fig. 5e), and with a peculiar of ramp-flat-ramp configuration.

A comparison of the two models at this final developments stage, i.e. when the upward- and downward-propagating faults are connected and the displacement produced by the two rigid blocks has reached the surface, shows significant differences.

SED
5, 2043–2079, 2013

Regarding fault geometry, we observed a listric profile in WK1 and a change in dip in WK2 coincident with the pre-existing low-angle discontinuity. Such ramp-flat-ramp profile in WK2 further stresses the role of the fault-bend folding mechanism connected to the growth of the upward-propagating fault, and, as a result, the bending moment faults in this experiment are more developed. Despite the rigidity of the blocks that simulate the hanging-wall and the footwall, the faulting evolution in WK1 and WK2 produced subsiding basins having different shape. Whereas the basin in WK1 is relatively flat, a bowl-shaped basin having its depocenter 40 mm far from the surface-breaking fault developed in WK2.

In summary, the results of the experiments show how strongly the mechanical discontinuity cut in the uniform material of the model affected the growth of the simulated master blind fault, delaying the upward propagation of the synthetic faults that developed from its tip. Both experiments showed that sub-vertical bending-moment faults are the first structures to form at the surface, as shown also by other analogue experiments (e.g. van Gent et al., 2010). In the wet kaolin experiments, such secondary structures mainly developed with a Mode I mechanism showing an excessive width (see for example the final step of WK2; Fig. 5g), probably due to the quite high cohesion of wet kaolin.

4.2 Quartz sand experiments

Although wet kaolin is very effective as an analogue material, its high cohesion may result in undesirable modeling effects. To overcome this limitation we reproduced some key features of the models obtained with the clay experiments using dry sand.

We performed two different experiments simulating only the rocks located above the upper tip of an master fault, assumed to be located at 3 km depth. The first experiment, Quartz Sand #1 (QS1), used the same experimental apparatus of the wet kaolin experiments, with two rigid blocks, one of which is mobile and acts as a subsiding hanging-wall fault block (Fig. 6a). This experiment was conceived to evaluate how much the rheological differences between wet kaolin and dry sand affect deformation

SED
5, 2043–2079, 2013

patterns. In the second experiment, Quartz Sand #2 (QS2), the hanging-wall fault block was replaced by a flexing plate connected to the stepper motor. The aim of this experiment was strictly to reproduce a basin with a depocenter shifted towards the center of the hanging-wall and located far from the hypothetical surface prolongation of a master fault dipping 45–50° (Fig. 6b). This configuration is reminiscent of both the position of the depocenter in the experiment WK1 and of the shape of the coseismic depression created by the L'Aquila earthquake. Therefore the model focuses specifically on the shallowest 3 km of the crust, i.e., on the rock volume that – if the master fault were dominantly blind – would be most affected by brittle deformation due to bending rather than by simple shearing.

The experiment used quartz sand having the following mechanical properties: cohesion 30 Pa, coefficient of internal friction 0.88, angle of internal friction 41°. Under these experimental conditions 1 cm in the model represents 0.5 km in nature.

The results of QS1 do not show remarkable differences with respect to WK1; the upward-propagating fault nucleates at the upper tip of the simulated master fault and it rapidly reaches the surface (Fig. 6c). Its associated basin is quite similar to that seen in WK1.

In QS2, a forced-fold developed above the tip of the hypothetical fault as a result of the imposed bending (Fig. 6d). A series of crestal fractures, some showing small but measurable vertical throw due to low cohesion of the dry sand, formed where the tensile stress is maximum, that is to say along the hypothetical up-dip prolongation of the master fault. Overall, these structures are reminiscent of the bending-moment faults recognized in the wet kaolin experiments.

5 Discussion

Our analogue models, especially WK2 and QS2, show the mechanical feasibility of a long-lived buried extensional master fault with disconnected secondary normal faults roughly lying along the same hypothetical plane. Model QS2 also demonstrates that

SED
5, 2043–2079, 2013

bending moment faults developed in a low cohesion material may display some vertical displacement, mimicking a genuine upward-propagating fault, and that the size and the shape of the basin related to the growth of upward-propagating faults depends on the growth rate of the faults.

It has long been known that non-elastic deformation of the rock volume around the main fault may reduce or impede fault propagation (e.g. Roering et al., 1997). It is also well known that when a propagating failure meets a mechanical discontinuity, such as a weak layer or a pre-existing fault, the failure may stop, penetrate it, or be deflected along it (e.g. Dyer, 1988).

Based on the available data about the L'Aquila sequence and on modeling results, we believe that the low-angle plane that exists at 3 km depth has played an active role in preventing coseismic slip from propagating to the surface, hence strongly affecting the mid- to long-term evolution of the shallow portion of the entire fault system.

Our results cast doubts on the nature of the surface fractures detected after the 2009 L'Aquila earthquake, in particular on the interpretation of the Paganica fault. In the following we discuss the available seismological and geological evidence in light of our modeling results for different portions of the fault system.

5.1 Paganica fault: upward-propagating or downward-propagating fault?

To address this question we move from the evidence supplied by the aftershock pattern. In this respect we wish to recall that, although very shallow aftershocks were imaged between 1 and 3 km depth near the northern end of the seismogenic source, no aftershocks where observed between the surface and 2–3 km depth in its central portion, i.e. near Paganica (Chiarabba et al., 2009; Chiaraluce et al., 2011; Chiaraluce, 2012; Valoroso et al., 2013). This could be well explained by the velocity strengthening behavior of faults at shallow crustal depth, that is to say, in the Upper Stability Transition zone (UST) defined by Scholz (1988), but two additional explanations are equally likely: (1) the normal stress acting on the uppermost part of the fault plane, which controls the effective coefficient of friction of the rupture, might be especially low, thus generating

SED
5, 2043–2079, 2013

stable sliding (e.g. Brace and Byerlee, 1970); or, more simply, (2) there is no fault plane continuity in the uppermost 2–3 km of the crust in the Paganica area. It is well known that the UST zone is not always found in seismogenic areas; for instance, Marone and Scholz (1988) investigated continental faults and concluded that the UST occurs only in mature fault zones: consequently, young faults and faults with long recurrence intervals or negligible gouge zones do not exhibit an UST zone.

Unfortunately, neither field nor trenching observations allow the nature of the Paganica fault gouge to be assessed, as the only available information consists of extensional and shear joints nearby Paganica village. There is simply no surface exposure of the Paganica fault which could be used to state whether or not this fault is well-developed at depth. Moreover, even if we considered the Paganica extensional and shear joints as secondary branches of the seismogenic source reaching the surface, we would expect slip along these features to result from velocity strengthening during afterslip, i.e. hours or days after the mainshock (e.g. Perfettini and Ampuero, 2008). Luckily, we know exactly the timing of surface breakage near Paganica, as the Paganica–Tempera aqueduct high-pressure pipe (crossing the Paganica fault not far from the village center) was reported broken during the mainshock (Vittori et al., 2011). Hence this effect is incompatible with afterslip along a secondary branch of the main seismogenic fault.

Our analogue models show the mechanical feasibility of a long-lived buried extensional master fault with disconnected secondary normal faults roughly lying along the same hypothetical plane. The proposed scheme reproduces satisfactorily all information available on the current setting and on the presumed evolution of the Paganica surface rupture. We hence interpret the Paganica breaks as corresponding to the tensional and shear joints that accommodate the deformation within the fold induced by the buried master fault.

5.2 Northern end of the L'Aquila fault system

With regard to the northern end of the activated fault system, the aftershock distribution indeed appears to delineate a master fault plane and its associated shallower

SED
5, 2043–2079, 2013

secondary structures (Fig. 3a). These may appear as secondary splays of a master fault approaching the surface. As shown by the results of the experiment WK2, however, this should imply that in this sector the fault system is more developed than in the central sector.

To test this hypothesis we related the central and northern sectors of the L'Aquila fault system (Fig. 3a and b) to distinct subsequent steps of the wet clay experiments. One could visually assign the central sector to the step shown in the Fig. 3d, and the northern sector to the step of Fig. 3g. Several observations, however, make this view questionable.

Seismological data, observations of surface co- and post-seismic deformation and inferences on the morphotectonic evolution of the Aterno River Valley, all indicate that the L'Aquila fault system generated the maximum displacement in its central portion, as it is seen in most fault systems worldwide (Fig. 3). As a consequence, also the secondary structures directly generated by the master fault should be more developed in the central sector, in contrast with all available observations.

A plausible explanation for this ambiguous configuration involves the reactivation of inherited extensional fault systems located close to the upper tip of the seismogenic blind master fault. As we mentioned in the description of local geological setting, the Abruzzi Apennines are the result of three subsequent deformation phases: Mesozoic extension, Cenozoic compression and shortening, and finally Plio-Quaternary extension. The high-angle faults that we see today at the surface may be related to any of these deformation events: for instance, they could be Mesozoic faults incorporated and translated within the Cenozoic thrust sheets, or perhaps normal faults developed in the backlimbs of thrust-related anticlines during Cenozoic compression (see Scisciani et al., 2002 for a review on this topic).

As we have shown, an inherited thrust plane is present at 3 km depth, therefore, some of the structures that we observed as a reactivated during the 2009 sequence may be related to the previous deformation phases. A feasible hypothesis about the nature of the faults system that we observe along the northern sector of the L'Aquila

SED
5, 2043–2079, 2013

system may provide a reactivation mechanism of inherited extensional fault systems fortuitously located near the upper tip of the seismogenic blind master fault.

We conclude suggesting that the coseismic slip confined at depth during the mainshock caused triggered motion on inherited extensional faults, i.e. the buried portion of the Mt. Stabiata and Aragno faults. It is well known that blind earthquake ruptures impart stress on the overlying crust, triggering any pre-existing faults (e.g. Lin and Stein, 2004). This hypothesis is supported by the post-seismic strain recovery observed just above this shallow structure (D'Agostino et al., 2012).

5.3 A down-dip segmentation scheme of the seismogenic source

We propose that the causative fault of the 2009 L'Aquila earthquake is confined at a depth > 3 km and that the complex interaction with inherited structures not only prevented coseismic slip from propagating to the surface, but also reduced the natural mid-to-long term tendency of the master fault to propagate to the surface. Accordingly, we interpret the Paganica breaks as corresponding to the tensional and shear joints that accommodate the deformation within the fold induced by the normal fault propagation.

We contend that also the lower seismicity cut-off (9–10 km), a further distinctive feature of the sequence, can be interpreted as due to the presence of another inherited thrust surface that, according to Atzori et al. (2013), may have played an important role during or immediately after the earthquake. Notice that while analyzing the northernmost portion of the 2009 aftershock sequence, Bigi et al. (2013) described a seismogenic normal fault confined by thrust faults inherited from a previous tectonic phase at both its bottom and its top. This further suggests that inherited thrust faults may play a significant role in the Central Apennines seismotectonics.

In summary, we propose a scheme that reproduces satisfactorily all information available on the current setting and on the presumed evolution of both the 2009 L'Aquila seismogenic fault and the Paganica surface ruptures. We suggest that the causative fault of the 2009 L'Aquila earthquake was segmented in the depth interval 3–10 km due

SED
5, 2043–2079, 2013

to the complex interaction with inherited structures. We believe that these limitations, which are due to permanent characteristics of the local geological setting, contributed to reduce the magnitude of the 2009 earthquake, and we expect to have done so also through previous seismic cycles.

6 Conclusions

Our analysis of seismogenic faulting in the L'Aquila area revealed an unprecedented complexity in the interaction between coseismic slip and inherited structural features. In particular, it suggests that the main surface coseismic rupture – the Paganica fault – can be better explained as a result of surface bending rather than as the direct prolongation of the seismogenic master fault. Under these circumstances, the length of the faulted zone and the extent of surface slip would be controlled more by the rheology of the shallow rocks that by slip at depth; this would ultimately prevent the surface rupture parameters from being used to derive the earthquake magnitude using empirical relationships (e.g. Wells and Coppersmith, 1994), both for the current event and for previous earthquakes detected through paleoseismological trenching. This conclusion explains both the hidden nature of the earthquake causative fault prior to 2009 and the wide scatter of the proposed rupture models (see Vittori et al., 2011; Vannoli et al., 2012, for a review).

The large density of faults in the region, coupled with a limited historical earthquake record, is perhaps at the basis of a "L'Aquila paradox" (Valensise, 2009). In a study based on a mixed geological-statistical approach (Akinci et al., 2009; published before the 6 April earthquake) the area of the future 2009 earthquake was given a relatively high probability of experiencing strong ground shaking in the following 50 yr. This conclusion was supported by the many seismogenic sources included in the input model; ironically though, the corresponding surface primary active faults did not include the Paganica fault because of its weak geomorphic expression. For the same reason the Paganica fault received little attention in studies carried out prior to 2009, some of

SED
5, 2043–2079, 2013

which referred to it as “uncertain or buried” (Geological Map of Italy, 2009) while others did not map it at all (Galadini and Galli, 2000).

We believe the L’Aquila earthquake illustrates well the nature of the interaction between the seismogenic rupture and other inherited structures at depth (e.g. buried thrust planes), the partial reactivation of inherited surface faults (e.g. Bazzano, Mt. Stabiata and Pettino faults), and the occurrence of pseudo-primary surface ruptures (Paganica fault). We contend that the “unusual” 6 April 2009 L’Aquila earthquake in fact illustrates a common style of complex tectonic deformation, implying that the number of unrecognized, blind or hidden seismogenic faults in Italy – and probably elsewhere – could be larger than previously thought. Driven by the current tectonic regime such faults break through a highly complex upper crust, interacting in various ways with the existing structural fabric. This may result in limitations of their size, reactivation of inherited faults and generation of new surface breaks. What is absolutely crucial for the geological reconnaissance work is that in the field these highly diverse faults may exhibit a reversed hierarchy, the most obvious being the least relevant in a fault-based seismic hazard assessment and vice-versa.

Based on these observations, we propose a new hierarchization scheme of active normal faults in structurally complex areas (Fig. 6). Our scheme includes five categories, listed in descending order of relevance for seismic hazard assessment:

I. **Seismogenic master faults** (e.g. the L’Aquila earthquake master fault): includes all faults capable of generating earthquakes of $M \geq 5.5$. They may or may not reach the surface and cause primary surface faulting, depending on their depth, on the slip distribution and on the presence of favorably oriented, inherited discontinuities in the host rocks (see II). They are the main players in the assessment of ground shaking hazard.

II. **Inherited subsurface faults** (e.g. the low angle thrusts shown in Fig. 6): includes faults generated during previous deformation phases. They may act passively and serve as segment boundaries, effectively limiting the magnitude of earthquakes

SED
5, 2043–2079, 2013

generated by the master fault, or they can be themselves the locus of large aftershocks. As such they may play a limited role in the assessment of ground shaking hazard. The same mechanical role may be played by generic discontinuities within the host-rocks.

III. **Fault-propagation induced secondary faults**: includes breaks that represent the brittle response of the shallowest portion of the crust to the upward propagation of the master fault. These secondary faults are normally arranged in a roughly triangular horse-tail pattern that includes synthetic and antithetic splays, all stemming from the upper tip of the master fault. They may cause sizable surface faulting hazard.

IV. **Bending-related secondary surface faults** (e.g. Paganica fault): includes breaks that are generated by the crustal bending taking place above the uppermost portion of the master fault. As such they are expected to (a) occur near the upward prolongation of the deeper master fault, thus simulating primary surface faulting, and (b) be restricted to the middle of the upper tip of the master fault, above the portion of the fault where slip is usually largest and bending is consequently tightest. Bending-moment faults are expected to nucleate at the surface and extend downward up to a depth controlled by the bending geometry. They may cause sizable and somehow unpredictable surface faulting hazard.

V. **Inherited surface faults** (e.g. Bazzano and Pettino faults): includes faults formed during previous deformation phases; in our case they correspond mostly to faults bounding piggy-back basins, or more in general accompanying the progression of thrusting during the emplacement of the Apennines chain. They are generally very evident in the field and may or may not be reactivated, depending on their location and geometry with respect to the coseismic strain pattern imposed by the master fault. They may be relevant to the assessment of ground shaking hazard due to fault-trapped waves (Calderoni et al., 2012), but owing to their clear visibility they can be easily taken into account, thus posing limited surface faulting hazard.

SED
5, 2043–2079, 2013

Faulting is a complex phenomenon at all spatial and temporal scales. In the Abruzzi Apennines this complexity arises largely from (1) the superposition of a young (< 1 Myr) extensional tectonic regime over the outcomes of a compressional regime that built the chain by progressive thrusting over a time scale of 5–10 Myr; (2) the similarity between tectonic features that represent the primary outcome of the ongoing extensional regime and secondary, inherited extensional features that are commonly associated with thrusting; and (3) the progressive rejuvenation by regional uplift, a fast landscape-building process which largely outpaces the ongoing regional extension and that is also responsible for generating fault-like gravity features. An extremely well-documented earthquake such as 2009 occurring in a relatively isolated intermontane depression such as the mid-Aterno Valley affords the rare possibility to investigate the interplay of these competing processes without being tricked by the appearances or – even more importantly – without being ruled by dogmas.

The work and the ideas we presented have obvious and important implications in the context of seismic hazard assessment. The "*. . . ability to distinguish between tectonically induced primary and secondary faulting, faulting induced by strong ground motions, and faulting induced by nontectonic phenomena. . .*" has been seen by Hanson et al. (1999) as a fundamental pre-requisite for devising appropriate regulatory criteria in the siting of nuclear power plants and other critical facilties. McCalpin (2000), among several others, has discussed strategies for the analysis of secondary features associated with the distributed expression of reverse faulting, including bending-moment faults, flexural-slip faults and folds, and has placed them into a hierarchical classification. Much of this work, however, deals with secondary faulting induced by positively blind faults in compressional environments, because this is the dominating tectonic style in the countries where these studies were initiated. So far there has been little appreciation for the fact that the same features and interpretative problems may be seen also in extensional environments: our study aims to fill this gap using the unique evidence from the 2009 earthquake.

SED
5, 2043–2079, 2013

Italy no longer has nuclear facilities in operation, but it is a highly seismic country that hosts a large fraction of the worldwide cultural heritage. Not all areas are equally at risk, hence any building retrofitting strategy requires priorities to be set based on careful examination of the true seismogenic potential of each individual seismogenic area. Much work has already been carried out on the potential of Italian faults, and several quiescent areas are being watched closely following the identification of presumed active tectonic features. The results of our analysis suggest that an objective evaluation of the hazard posed by any proposed active fault requires full and proper appreciation of its true hierarchy level. This is to be achieved by blending surface, subsurface, geomorphic, structural and seismological data and, more importantly, by avoiding preconceptions and overly simplified models.

Acknowledgements. This work was financially supported by Regione Lombardia, by the Italian Ministry of Research and Education (MIUR) in the frame of INGV's Progetto Abruzzo, and by Presidenza del Consiglio dei Ministri – Dipartimento della Protezione Civile (DPC). The views and conclusions contained in this paper are those of the authors and should not be interpreted as necessarily representing official opinions and policies, either expressed or implied, of the Italian Government.

References

Akinci, A., Galadini, F., Pantosti, D., Petersen, M., Malagnini, L., and Perkins, D.: Effect of time dependence on probabilistic seismic-hazard maps and deaggregation for the Central Apennines, Italy, B. Seismol. Soc. Am., 99, 585–610, 2009.

Anzidei, M., Boschi, E., Cannelli, V., Devoti, R., Esposito, A., Galvani, A., Melini, D., Pietrantonio, G., Riguzzi, F., Sepe, V., and Serpelloni, E.: Coseismic deformation of the destructive April 6, 2009 L'Aquila earthquake (central Italy) from GPS data, Geophys. Res. Lett., 36, L17307, doi:10.1029/2009GL039145, 2009.

Atzori, S., Hunstad, I., Chini, M., Salvi, S., Tolomei, C., Bignami, C., Stramondo, S., Trasatti, E., Antonioli, A., and Boschi, E.: Finite fault inversion of DInSAR coseismic dis-

SED
5, 2043–2079, 2013

placement of the 2009 L'Aquila earthquake (central Italy), Geophys. Res. Lett., 36, L15305, doi:10.1029/2009GL039293, 2009.
Atzori, S., Chiarabba, C., Devoti, R., Bonano, M., and Lanari, R.: Anomalous far-field geodetic signature related to the 2009 L'Aquila (central Italy) earthquake, Terra Nova, doi:10.1111/ter.12040, 2013.
Bagnaia, R., D'Epifanio, A., and Labini, S. S.: Aquilan and Subaequan basins: an example of Quaternary evolution in central Apennines, Italy, Quaternaria Nova, 2, 187–209, 1992.
Basili, R., Bosi, V., Galadini, F., Galli, P., Meghraoui, M., Messina, P., Moro, M., and Sposato, A.: The Colfiorito earthquake sequence of September–October 1997: surface breaks and seismotectonic implications for the central Apennines (Italy), J. Earthq. Eng., 2, 291–302, 1998.
Bianchi, I., Chiarabba, C., and Piana Agostinetti, N.: Control of the 2009 L'Aquila earthquake, central Italy, by a high-velocity structure: a receiver function study, J. Geophys. Res., 115, B12326, doi:10.1029/2009JB007087, 2010.
Bigi, S., Casero, P., Chiarabba, C., and Di Bucci, D.: Contrasting surface active faults and deep seismogenic sources unveiled by the 2009 L'Aquila earthquake sequence (Italy), Terra Nova, 25, 21–29, doi:10.1111/ter.12000, 2013.
Boncio, P., Pizzi, A., Brozzetti, F., Pomposo, G., Lavecchia, G., Di Naccio, D., and Ferrarini, F.: Coseismic ground deformation of the 6 April 2009 L'Aquila earthquake (central Italy, Mw 6.3), Geophys. Res. Lett., 37, L06308, doi:10.1029/2010GL042807, 2010.
Bonini, L., Di Bucci, D., Toscani, G., Seno, S., and Valensise, G.: Reconciling deep seismogenic and shallow active faults through analogue modeling; the case of the Messina Straits (southern Italy), J. Geol. Soc. London, 168, 191–199, 2011.
Brace, W. F. and Byerlee, J. D.: California earthquakes: why only shallow focus?, Science, 168, 1573–1575, 1970.
Calamita, F., Satolli, S., Scisciani, V., Esestime, P., and Pace, P.: Contrasting styles of fault reactivation in curved orogenic belts: examples from the Central Apennines (Italy), Geol. Soc. Am. Bull., 123, 1097–1111, 2011.
Calderoni, G., Di Giovambattista, R., Vannoli, P., Pucillo, S., and Rovelli, A.: Fault-trapped waves depict continuity of the fault system responsible for the 6 April 2009 MW 6.3 L'Aquila earthquake, central Italy, Earth Planet. Sc. Lett., 323–324, 1–8, 2012.
Carafa, M. M. C. and Barba, S.: The stress field in Europe: optimal orientations with confidence limits, Geophys. J. Int., 193, 531–548, doi:10.1093/gji/ggt024, 2013.

SED
5, 2043–2079, 2013

Chiarabba, C., Amato, A., Anselmi, M., Baccheschi, P., Bianchi, I., Cattaneo, M., Cecere, G., Chiaraluce, L., Ciaccio, M. G., De Gori, P., De Luca, G., Di Bona, M., Di Stefano, R., Faenza, L., Govoni, A., Improta, L., Lucente, F. P., Marchetti, A., Margheriti, L., Mele, F., Michelini, A., Monachesi, G., Moretti, M., Pastori, M., Piana Agostinetti, N., Piccinini, D., Roselli, P., Seccia, D., and Valoroso, L.: The 2009 L'Aquila (central Italy) MW 6.3 earthquake: main shock and aftershocks, Geophys. Res. Lett., 36, L18308, doi:10.1029/2009GL039627, 2009.

Chiarabba, C., Bagh, S., Bianchi, I., De Gori, P., and Barchi, M.: Deep structural heterogeneities and the tectonic evolution of the Abruzzi region (Central Apennines, Italy) revealed by microseismicity, seismic tomography, and teleseismic receiver functions, Earth Planet. Sc. Lett., 295, 462–476, 2010.

Cheloni, D., D'Agostino, N., D'Anastasio, E., Avallone, A., Mantenuto, S., Giuliani, R., Mattone, M., Calcaterra, S., Gambino, P., Dominici, D., Radicioni, F., and Fastellini, G.: Coseismic and initial post-seismic slip of the 2009 Mw 6.3 L'Aquila earthquake, Italy, from GPS measurements, Geophys. J. Int., 181, 1539–1546, 2010.

Chiaraluce, L.: Unravelling the complexity of Apenninic extensional fault systems: a review of the 2009 L'Aquila earthquake (Central Apennines, Italy), J. Struct. Geol., 42, 2–18, 2012.

Chiaraluce, L., Valoroso, L., Piccinini, D., Di Stefano, R., and De Gori, P.: The anatomy of the 2009 L'Aquila normal fault system (central Italy) imaged by high resolution foreshock and aftershock locations, J. Geophys. Res., 116, B12311, doi:10.1029/2011JB008352, 2011.

Cloos, E.: Experimental analysis of Gulf Coast fracture patterns, AAPG Bull., 52, 420–444, 1968.

Cooke, M. L. and van der Elst, N. J.: Rheologic testing of wet kaolin reveals frictional and bi-viscous behaviour typical of crustal materials, Geophys. Res. Lett., 39, L01308, doi:10.1029/2011GL050186, 2012.

Cooke, M. L., Schottenfeld, M. T., and Buchanan, S. W.: Evolution of fault efficiency at restraining bends within wet kaolin analog experiments, J. Struct. Geol., 51, 180–192, 2013.

D'Agostino, N., Mantenuto, S., D'Anastasio, E., Giuliani, R., Mattone, M., Calcaterra, S., Gambino, P., and Bonci, L.: Evidence for localized active extension in the central Apennines (Italy) from Global Positioning System observation, Geology, 39, 291–294, 2011.

D'Agostino, N., Cheloni, D., Fornaro, G., Giuliani, R., and Reale, D.: Space-time distribution of afterslip following the 2009 L'Aquila earthquake, J. Geophys. Res., 117, B02402, doi:10.1029/2011JB008523, 2012.

SED
5, 2043–2079, 2013

D'Anastasio, E., De Martini, P. M., Selvaggi, G., Pantosti, D., Marchioni, A., and Maseroli, R.: Short-term vertical velocity field in the Apennines (Italy) revealed by geodetic levelling data, Tectonophysics, 418, 219–234, 2006.

Di Stefano, R., Chiarabba, C., Chiaraluce, L., Cocco, M., De Gori, P., Piccinini, D., and Valoroso, L.: Fault zone properties affecting the rupture evolution of the 2009 (M_w 6.1) L'Aquila earthquake (central Italy): Insights from seismic tomography, Geophys. Res. Lett., 38, L10310, doi:10.1029/2011GL047365, 2011.

Dyer, R.: Using joint interactions to estimate paleostress ratios, J. Struct. Geol., 10, 685–699, 1988.

Eisenstadt, G. and Sims, D.: valuating sand and clay models; do rheological differences matter?, J. Struct. Geol., 27, 1399–1412, 2005.

Emergeo Working Group: Evidence for surface rupture associated with the Mw 6.3 L'Aquila earthquake sequence of April 2009 (central Italy), Terra Nova, 22, 43–51, 2010.

Erslev, E. A.: Trishear fault-propagation folding, Geology, 19, 617–620, doi:10.1130/0091-7613(1991)019<0617:TFPF>2.3.CO;2,1991.

Galadini, F.: Pleistocene changes in the central Apennine fault kinematics: a key to decipher active tectonics in central Italy, Tectonics, 18, 877–894, 1999.

Galadini, F. and Galli, P.: Active tectonics in the Central Apennines (Italy) – input data for seismic hazard assessment, Nat. Hazards, 22, 225–268, 2000.

Galadini, F., Meletti, C., and Vittori, E., Stato delle conoscenze sulle faglie attive in Italia: elementi geologici di superficie, in: Le Ricerche Del GNDT Nel Campo Della Pericolosità Sismica (1996–1999), edited by: Galadini, F., Meletti, C., and Rebez, A., CNR-GNDT, Gruppo Nazionale per la Difesa dai Terremoti, Roma, Italy, 107–136, 2000.

Geological Map of Italy: L'Aquila sheet, n. 359, 1 : 50 000 scale, available at: http://www.isprambiente.gov.it/MEDIA/carg/359_LAQUILA/Foglio.html, 2009.

Gori, S., Falcucci, E., Atzori, S., Chini, M., Moro, M., Serpelloni, E., Fubelli, G., Saroli, M., Devoti, R., Stramondo, S., Galadini, F., and Salvi, S.: Constraining primary surface rupture length along the Paganica fault (2009 L'Aquila earthquake) with geological and geodetic (DInSAR and GPS) data, Italian Journal of Geosciences, doi:10.3301/IJG.2012.21, 2012.

Hanson, K. L., Kelson, K. I., Angell, M. A., and Lettis, W. R.: Techniques for identifying faults and determining their origins, NUREG/CR-5503, US Nuclear Regulatory Commission, 1999.

Hardy, S. and Ford, M.: Numerical modeling of trishear fault propagation folding, Tectonics, 16, 841–854, doi:10.1029/97TC01171, 1997.

SED
5, 2043–2079, 2013

Henza, A., Withjack, M. O., and Schlische, R. W.: Normal-fault development during two phases of non-coaxial extension: an experimental study, J. Struct. Geol., 32, 1656–1667, doi:10.1016/j.jsg.2009.07.007, 2010.
Herrmann, R. B., Malagnini, L., and Munafò, I.: Regional moment tensors of the 2009 L'Aquila earthquake sequence, Bull. Seismol. Soc. Am., 101, 975–993, 2011.
Hyppolite, J.-C., Angelier, J., and Roure, F.: A major geodynamic change revealed by Quaternary stress patterns in the Southern Apennines (Italy), Tectonophysics, 230, 199–210, 1994.
Hubbert, M. K.: Theory of scale models as applied to the study of geologic structures, Geol. Soc. Am. Bull., 48, 1459–1520, 1937.
Improta, L., Villani, F., Bruno, P. P., Castiello, A., De Rosa, D., Varriale, F., Punzo, M., Brunori, C. A., Civico, R., Pierdominici, S., Berlusconi, A., and Giacomuzzi, G.: High-resolution controlled-source seismic tomography across the Middle Aterno Basin in the epicentral area of the 2009, Mw 6.3, L'Aquila earthquake (central Apennines, Italy), Italian Journal of Geosciences, 131, 373–388, 2012.
Jin, G. and Groshong Jr., R. H.: Trishear kinematic modeling of extensional fault-propagation folding, J. Struct. Geol., 28, 170–183, 2006.
Kim, Y.-S. and Sanderson, D. J.: The relationship between displacement and length of faults: a review, Earth-Sci. Rev., 68, 317–334, 2005.
Lavecchia, G., Ferrarini, F., Brozzetti, F., De Nardis, R., Boncio, P., and Chiaraluce, L.: From surface geology to aftershock analysis: constraints on the geometry of the L'Aquila 2009 seismogenic fault system, Italian Journal of Geosciences, 131, 330–347, doi:10.3301/IJG.2012.24, 2012.
Lin, J. and Stein, R. S.: Stress triggering in thrust and subduction earthquakes and stress interaction between the southern San Andreas and nearby thrust and strike-slip faults, J. Geophys. Res., 109, B02303, doi:10.1029/2003JB002607, 2004.
McCalpin, J. P.: Paleoseismology, 2nd edn., Academic Press, 647 pp., 2009.
Marone, C. and Scholz, C. H.: The depth of seismic faulting and the upper transition from stable to unstable slip regimes, Geophys. Res. Lett., 15, 621–624, 1988.
Miller, J. F. and Mitra, S.: Deformation and secondary faulting associated with basement-involved compressional and extensional structures, AAPG Bull., 95, 675–689, 2011.
Montone, P., Mariucci, M. T., and Pierdominici, S.: The Italian present-day stress map, Geophys. J. Int., 189, 705–716, 2012.

SED
5, 2043–2079, 2013

Pace, B., Peruzza, L., Lavecchia, G., and Boncio, P.,: Layered seismogenic source model and probabilistic seismic-hazard analyses in Central Italy, Bull. Seism. Soc. Am., 96, 107–132, 2006.
Patacca, E. and Scandone, P.,: Post-Tortonian mountain building in the Apennines. The role of the passive sinking of a relic lithospheric slab, in: The Lithosphere in Italy, edited by: Boriani, A., Bonafede, M., Piccardo, G. B., and Vai, G. G., Accademia dei Lincei, Roma, 157–176, 1989.
Perfettini, H. and Ampuero, J.-P.: Dynamics of a velocity strengthening fault region: implications for slow earthquakes and postseismic slip, J. Geophys. Res., 113, doi:10.1029/2007JB005398, 2008.
Roering, J., Cooke, M. L., and Pollard, D.: Why blind thrust faults do not propagate to the Earth's surface: numerical modeling of coseismic deformation associated with thrust-related anticlines, J. Geophys. Res., 102, 11901–11912, doi:10.1029/97JB00680, 1997.
Schellart, W. P.: Shear test results for cohesion and friction coefficients for different granular materials: scaling implications for their usage in analogue modeling, Tectonophysics, 324, 1–16, 2000.
Scholz, C. H.: The brittle-plastic transition and the depth of seismic faulting, Geol. Rundsch., 77, 319–328, 1988.
Scisciani, V., Tavarnelli, E., and Calamita, F.: The interaction of extensional and contractional deformations in the outer zones of the Central Apennines, Italy, J. Struct. Geol., 24, 1647–1658, 2002.
Scognamiglio, L., Tinti, E., Michelini, A., Dreger, D. S., Cirella, A., Cocco, M., Mazza, S., and Piatanesi, A.: Fast determination of moment tensors and rupture history: what has been learned from the 6 April 2009 L'Aquila earthquake sequence, Seismol. Res. Lett., 81, 892–906. 2010.
Servizio Geologico d'Italia: Sheet #359 L'Aquila, of Carta Geologica d'Italia, scale 1 : 50 000, SELCA, Florence, Italy, 2006.
Stirling, M., Goded, T., Berryman, K., and Litchfield, N.: Selection of earthquake scaling relationships for seismic-hazard analysis, B. Seismol. Soc. Am., 103, 1–19, 2013.
van Gent, H. W., Holland, M., Urai, J. L., and Loosveld, R.: Evolution of fault zones in carbonates with mechanical stratigraphy – insights from scale models using layered cohesive powder, J. Struct. Geol., 32, 1375–1391, 2010.

SED
5, 2043–2079, 2013

Valensise, G.: Faglie attive e terremoti: tempo di cambiare strategie, Geoitalia, 28, 12–17, available at: http://www.geoitalia.org/upload/home_page/geoitalia/n28.pdf, 2009.
Valensise, G. and Pantosti, D.: The investigation of potential earthquake sources in peninsular Italy: a review, J. Seismol., 5, 287–306, 2001.
Valoroso, L., Chiaraluce, L., Piccinini, D., Di Stefano, R., Schaff, D., and Waldhauser, F.: Radiography of a normal fault system by 64,000 high-precision earthquake locations: the 2009 L'Aquila (central Italy) case study, J. Geophys. Res., 118, 1156–1176, doi:10.1002/jgrb.50130, 2013.
Vannoli, P., Burrato, P., Fracassi, U., and Valensise, G.: A fresh look at the seismotectonics of the Abruzzi (Central Apennines) following the 6 April 2009 L'Aquila earthquake (Mw 6.3), Italian Journal of Geosciences, 131, 309–329, 2012.
Vezzani, L., Festa, A., and Ghisetti, F.: Geological-structural map of the Central-Southern Apennines (Italy), 1 : 250 000 scale, SELCA, Firenze, 2009.
Vittori, E., Di Manna, P., Blumetti, A. M., Comerci, V., Guerrieri, L., Esposito, E., Michetti, A. M., Porfido, S., Piccardi, L., Roberts, G. P., Berlusconi, A., Livio, F., Sileo, G., Wilkinson, M., McCaffrey, K. J. W., Phillips, R. J., and Cowie, P. A.: Surface faulting of the 6 April 2009 Mw 6.3 L'Aquila earthquake in Central Italy, B. Seismol. Soc. Am., 101, 4, 1507–1530, 2011.
Walters, R. J., Elliott, J. R., D'Agostino, N., England, P. C., Hunstad, I., Jackson, J. A., Parsons, B., Phillips, R. J., and Roberts, G.: The 2009 L'Aquila earthquake (central Italy): a source mechanism and implications for seismic hazard, Geophys. Res. Lett., 36, L17312, doi:10.1029/2009GL039337, 2009.
Wells, D. L. and Coppersmith, K. J.: New empirical relationships among magnitude, rupture length, rupture width, rupture area, and surface displacement, B. Seismol. Soc. Am., 84, 974–1002, 1994.
Wesnousky, S. G.: Displacement and geometrical characteristics of earthquake surface ruptures: Issues and implications for seismic hazard analysis and the earthquake rupture process, B. Seismol. Soc. Am., 98, 1609–1632, 2008.
Wilkinson, M., McCaffrey, K. J. W., Roberts, G. P., Cowie, P. A., Phillips, R. J., Michetti, A., Vittori, E., Guerrieri, L., Blumetti, A. M., Bubeck, A., Yates, A., and Sileo, G.: Partitioned postseismic deformation associated with the 2009 Mw 6.3 L'Aquila earthquake surface rupture measured using a terrestrial laser scanner, Geophys. Res. Lett., 37, L10309, doi:10.1029/2010GL043099, 2010.

SED
5, 2043–2079, 2013

Withjack, M. O. and Jamison, W. R.: Deformation produced by oblique rifting, Tectonophysics, 126, 99–124, doi:10.1016/0040-1951(86)90222-2, 1986.
Withjack, M. O. and Schlische, R. W.: Geometric and experimental models of extensional fault-bend folds, Geol. Soc. Spec. Pub., 253, 285–305, 2006.

SED
5, 2043–2079, 2013

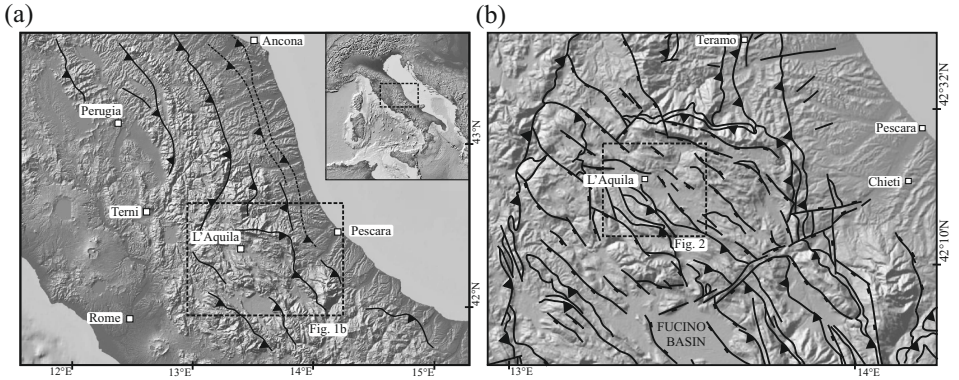

Fig. 1. (a) Digital Elevation Model of the Central Apennines, showing the trend of the main thrust fronts. A number of secondary fronts are also clearly delineated by the topography. **(b)** Tectonic map of the Abruzzi region (modified from Vezzani et al., 2009). The present morphology of the axial portion of the Apennines is still dominated by the folding and thrusting through which the chain was built up over a long time interval between the upper Miocene and the middle Pleistocene. Subsequent extension and intervening sedimentation in intermontane basins has so far only slightly modified the compressional architecture of the Apennines. A dashed box indicates the exact location of the study area.

SED
5, 2043–2079, 2013

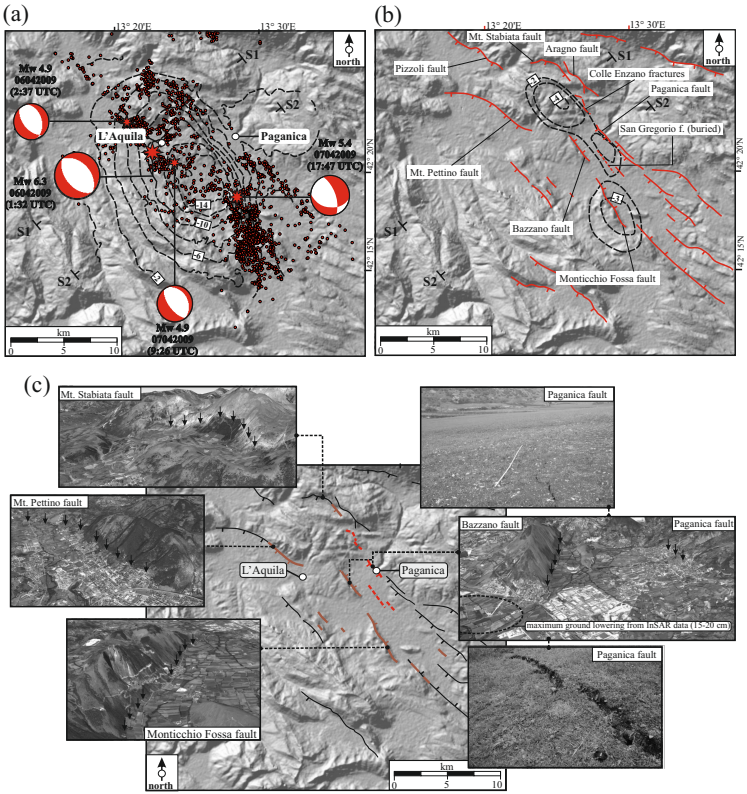

Fig. 2. **(a)** Map view of the L'Aquila area showing the location (red stars) and focal mechanisms of the largest events of the 2009 sequence (Scognamiglio et al., 2010). Dashed lines are contours of elevation changes observed between 4 and 12 April 2009 (D'Agostino et al., 2012). Red dots indicate relocated aftershocks (Chiaraluce et al., 2011). **(b)** Presumed active faults, shown by red lines. S1, S2 indicate the traces of cross sections 1 and 2. Dashed lines are contours of the elevation changes observed between 12 April and 5 October 2009 (D'Agostino et al., 2012). **(c)** Faults reported reactivated during the 2009 earthquake. Those shown in red are discontinuous fractures; black lines are presumed active faults and brown segments represent the portion of the faults reported as partially reactivated in 2009 (Emergeo Working Group, 2010). The insets show landscape views of the area (2× vertical exaggeration). On the right, two details of the surface ruptures along the Paganica fault are shown (Emergeo Working Group, 2010).

SED
5, 2043–2079, 2013

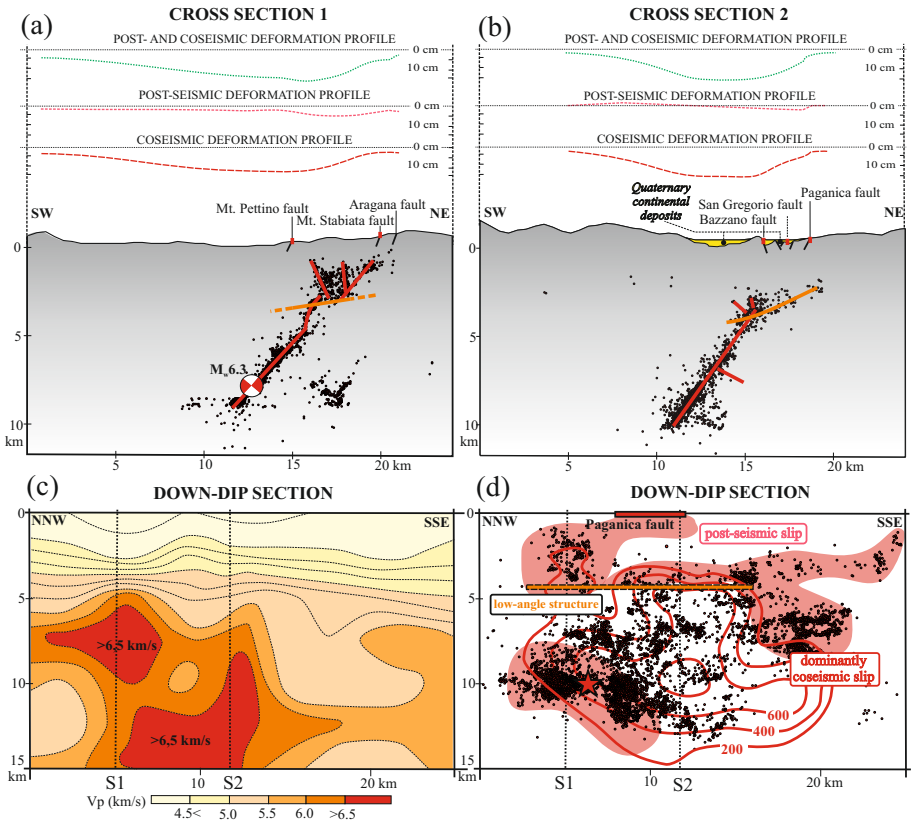

Fig. 3. **(a, b)** Cross sections, showing dominantly coseismic (4–12 April 2009; D'Agostino et al., 2012), post seismic (12 April–5 October 2009; D'Agostino et al., 2012) and cumulative elevation changes measured along the section trace. In all figures red dots indicate relocated aftershocks (Valoroso et al., 2013). Section traces are shown in Fig. 2. **(c, d)** Down-dip sections along the L'Aquila master fault (strike N135E; dip 50° to the WSW): **(c)** shows Vp values imaged along the fault plane (from Di Stefano et al., 2011); **(d)** shows the mainshock location (star). Red dots are aftershocks located within 0.5 km of the fault plane (Chiaraluce et al., 2011). Coseismic slip pattern, shown by red lines (contour interval is 200 mm; Atzori et al., 2009) and location of the inferred inherited thrust faults (orange thick lines). Red areas mark portions of the fault that experienced post-seismic slip (modified from D'Agostino et al., 2012).

SED
5, 2043–2079, 2013

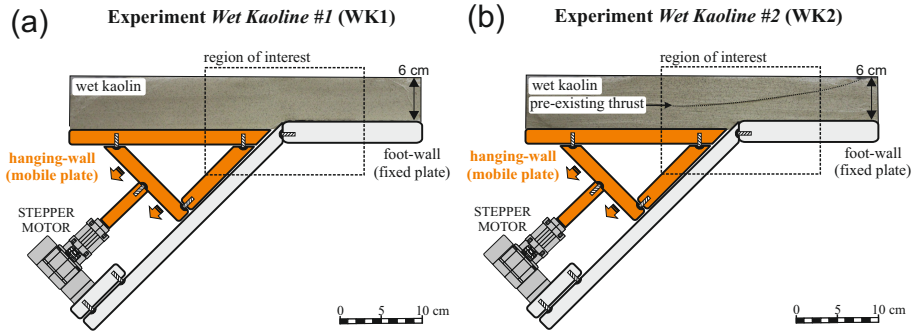

Fig. 4. Experimental setup used to model **(a)** a fault evolving in a homogeneous configuration and **(b)** with a low-angle discontinuity.

SED
5, 2043–2079, 2013

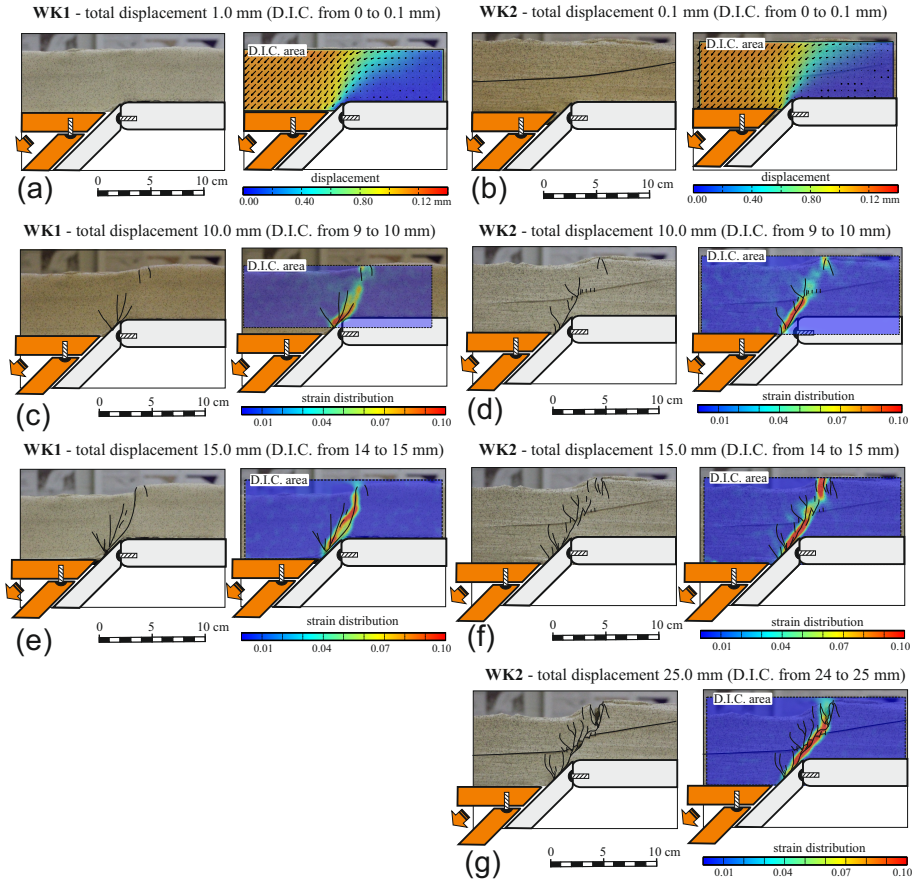

Fig. 5. Progressive evolution of the fault patterns in the wet clay experiments WK1 and WK2. For each step the brittle and ductile deformations have been analyzed using D.I.C witch returned the displacement field (**a** and **d**) and the strain distribution (from **c** to **g**).

SED
5, 2043–2079, 2013

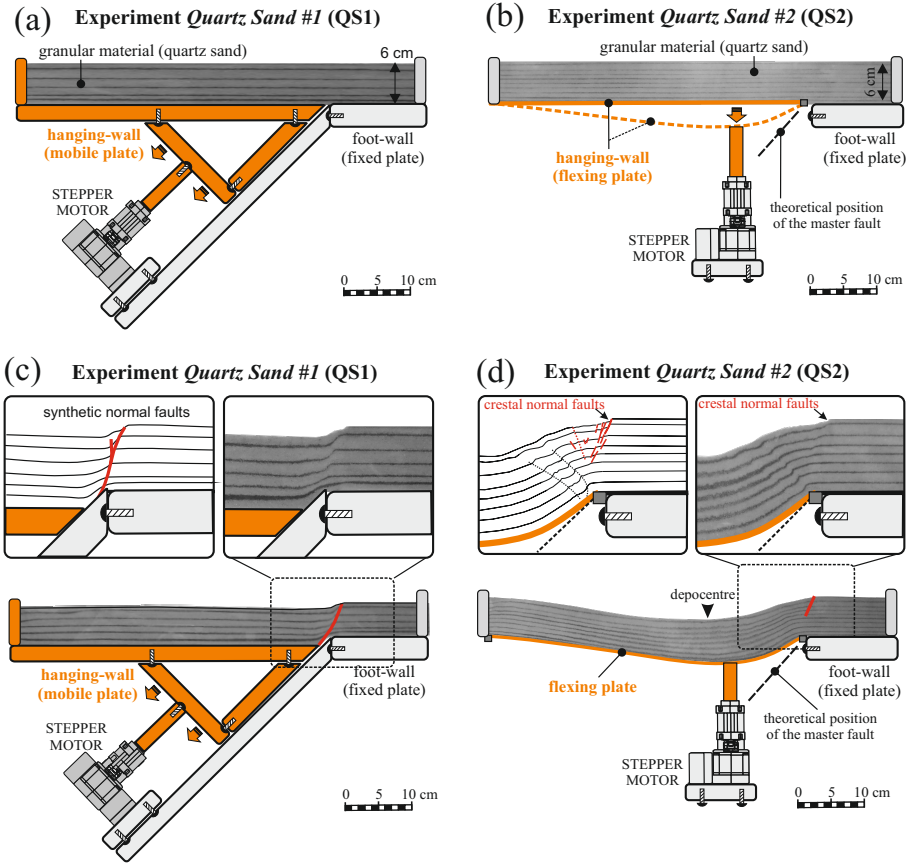

Fig. 6. Analogue modeling setup and results of the dry sand experiments QS1 and QS2. **(a)** and **(b)** are sketches of the experimental modeling apparatus. A dashed line in **(b)** and **(d)** indicates the theoretical position of the master (seismogenic) fault. **(c)** and **(d)** show the results of the experiment. Red lines represent newly formed faults.

SED
5, 2043–2079, 2013

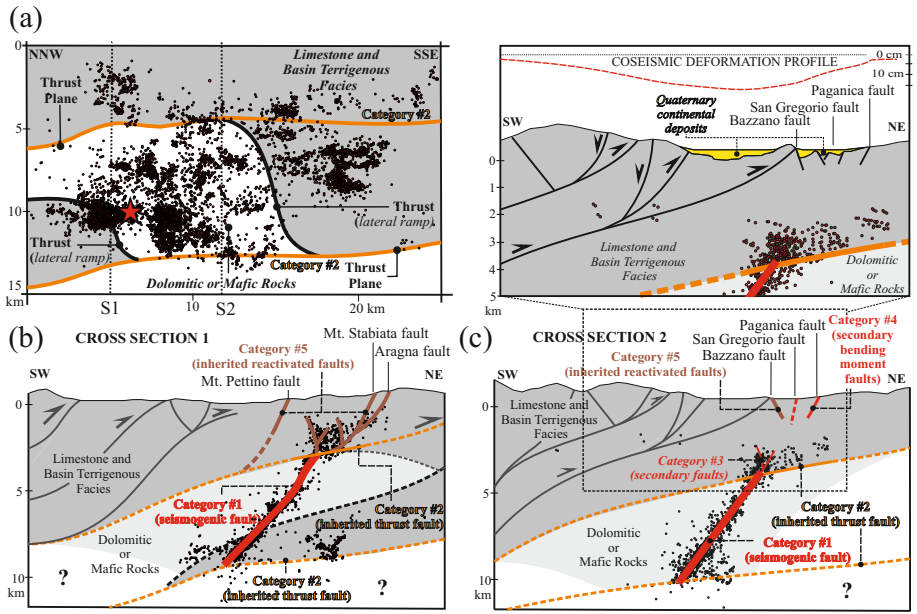

Fig. 7. (a) Distribution of the geological units along the down-dip section inferred based on Vp values. Black lines represent the inferred thrust fault cut by the section. **(b)** and **(c)** show section 1 and section 2 across two portions of the seismogenic fault. The figure shows also mainshock rupture (thick red lines), secondary faults whose activity was triggered by the mainshock (brown lines), the Paganica fault, and the geometry of the active faults not directly connected to the main seismogenic fault. Inset is a close-up view of cross-section **(b)**: the buried shape of the Quaternary basin (Improta et al., 2013), and dominantly coseismic elevation changes (dashed red line). In all figures red dots indicate relocated aftershocks (Valoroso et al., 2013). Section traces are shown in Fig. 2.

SED
5, 2043–2079, 2013